

Impact of Aromatic Compounds on Acid Gas Injection: Experimental Measurements and Predictions with the GC-PR-CPA Equation Of State

M. Hajiw¹, C. Coquelet¹, A. Chapoy^{1,2*}

¹*Mines ParisTech, PSL Research University, CTP – Centre of Thermodynamics of Processes, 35 rue Saint Honoré, 77305 Fontainebleau Cedex, France,*

²*Hydrates, Flow Assurance & Phase Equilibria Research Group, Institute of Petroleum Engineering, Heriot-Watt University, Edinburgh EH14 4AS, Scotland, United Kingdom*

* Corresponding author: a.chapoy@hw.ac.uk

Abstract

As more new fields contain high concentrations of carbon dioxide and hydrogen sulphide, there is a requirement for accurate equilibrium data for systems containing CO₂ and/or H₂S. Acid gases are undesirable and they are removed from the hydrocarbon stream after gas processing. They can be re-injected into the reservoir to enhance gas/oil recovery. However some hydrocarbons (e.g. methane and ethane) and aromatic compounds (e.g. benzene and toluene) may remain in the acid gases stream, becoming undesirable impurities leading to operation issues.

Accurate experimental measurements of hydrate dissociation points are essential to validate predictions of thermodynamic models. Although there is a significant amount of data available for sweet gas there is still a requirement for measurements for sour gas systems. Experimental measurements, vapour-liquid and vapour-liquid-liquid equilibria or hydrate dissociation conditions, have been conducted for different mixtures of hydrocarbons containing CO₂ and/or H₂S in high concentration. The GC-PR-CPA and SRK72-CPA were used in this work to predict the different phase equilibria of systems with acid gases and the hydrate-forming conditions are modelled by the solid solution theory of van der Waals and Platteeuw. The results reveal that our model is in good agreement with experimental data.

Introduction

About 40% of the untapped world's natural gas resources contain significant concentrations of carbon dioxide and hydrogen sulphide. Acid gases are undesirable and stripped from the hydrocarbon stream. A way to remove them is chemical absorption with various types of alkanolamines. After the amine regeneration process, acid gases come out at low pressure. Acid gases obtained are mainly made up of carbon dioxide and hydrogen sulphide but some light hydrocarbons and aromatic compounds might remain, becoming undesirable impurities leading to operation issues. Acid gases are also saturated with water at these conditions, leading to potential hydrates formation in pipelines. Sulphur recovery is usually not the best solution because of costly processes and environmental concerns make the practice of flaring acid gases undesirable. Therefore, acid gases injection into a suitable underground zone becomes the best solution. However, the impact of the different impurities on process operations is not very well known, due to the complexity of the mixtures. Indeed, a bibliographic study reveals that existing data are limited especially for multi-component systems containing acid gases.

Thus, experimental measurements, vapour-liquid equilibria and hydrate dissociation conditions, have been conducted for different mixtures containing CO₂ and/or H₂S. Hydrate dissociation points have been measured using the isochoric step-heating method for eight systems. The ratio between H₂S and CO₂ varied from 0% of H₂S to 75%. Different concentrations of hydrocarbons (methane, ethane, propane, benzene, toluene, m-xylene and cyclopentane) were added to evaluate their impact on the hydrate dissociation conditions (ratio gas to liquid from 25:1 to 1:1). Measurements were conducted in a cell made of Hastelloy C276 with a volume of 120 cm³. The setup can operate up to 40 MPa and between 203 and 323 K. The cell is immersed in a temperature controlled bath. To achieve a fast thermodynamic equilibrium device high pressure magnetic stirrer is used.

Comparing the different mixtures, the following observations can be made

- The presence of H₂S promotes hydrates formation and displaces the hydrate dissociation curve to higher temperatures (closer the pure H₂S curve)
- The presence of aromatic compounds tends to displace hydrate dissociation curves to lower temperatures. There is a difference of about 5 K between a ratio gas to liquid 5:1 and 1:1.

Accurate phase diagrams are of a great importance for process design. These diagrams can be predicted by equations of state. In this work, the GC-PR-CPA and SRK72-CPA equations of state (EoS) were used to predict the different phase equilibria of systems with acid gases [1,2]. These models result from the sum of two terms: a cubic equation of state and an associative term to take into account hydrogen bonding. There are thus particularly adapted for systems with water. In the GC-PR-CPA EoS, the Peng-Robinson cubic equation of state has been implemented. The second difference between both models is binary interaction parameters. While for the SRK72-CPA EoS, binary interaction parameters are polynomial functions adjusted for each binary system, the GC-PR-CPA is a group contribution method, where parameters are adjusted for different groups.

As for the hydrate phase modelling, these models were coupled with the van der Waals and Platteuw model [3], as implemented by Parrish and Prausnitz [4]. Both GC-PR-CPA and SRK72-CPA models are found to be in good agreement with experimental data.

Experimental Measurements

Hydrate dissociation points have been measured using the isochoric step-heating method. The apparatus is presented in Figure 1. The equilibrium setup consists of a cell made of Hastelloy C276 with a volume of 120 cm³. It can operate up to 40 MPa and between 203 and 323 K. The cell is immersed in a temperature controlled bath. To achieve a fast thermodynamic equilibrium device high pressure magnetic stirrer is used. A full description of the experimental setups and procedures can be found in the GPA Research-Report 230 [5].

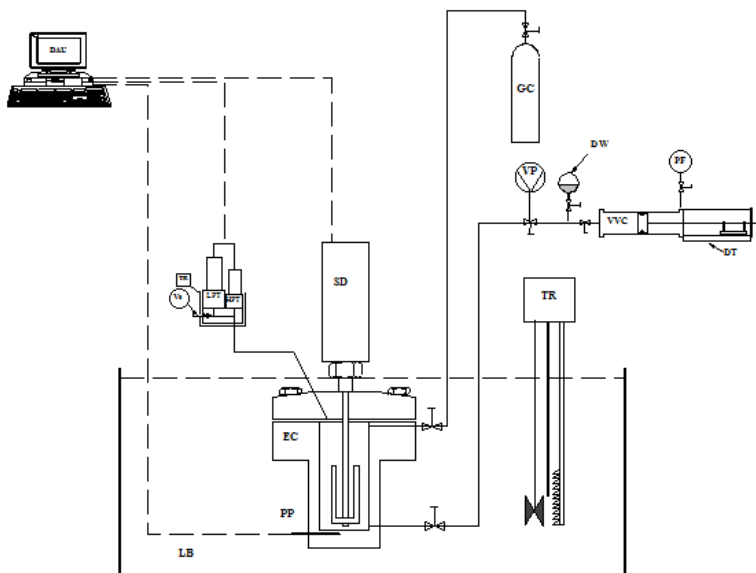


Figure 1: Schematic flow diagram of the apparatus. DW: degassed water; DAU: data acquisition unit; EC: equilibrium cell; GC: Gas cylinder; LPT: low pressure transducer; LPT: high pressure transducer; LB: liquid bath; PP: platinum probe; SD: stirring device; TR: temperature regulator; VP: vacuum pump; VVC: variable volume cell; PF: pressurizing fluid; DT: displacement transducer.

Thermodynamic Modelling

Two predictive models are used to predict phase equilibria for acid gases. Both have been developed on data for binary systems. Their capacity to predict phase equilibria for multi-component systems is tested in this paper. Group interaction parameters for the PPR78 EoS can be found in the paper by Xu et al. [6]. As for the GC-PR-CPA EoS, it is first necessary to adjust PR-CPA parameters for pure water. They have been adjusted on vapour pressure and saturated liquid density data. They are recall listed in Table 1. The PR – CPA EoS is expressed here, in term of pressure:

$$P = \frac{RT}{v - b_i^{PR}} - \frac{a_i(T)}{v(v + b_i^{PR}) + b_i^{PR}(v - b_i^{PR})} - \frac{1}{2} \frac{RT}{v} \left(1 + \rho \frac{\partial \ln(g)}{\partial \rho} \right) \sum_{i=1}^N x_i \sum_{A_i} (1 - X^{A_i})$$

Group interaction parameters for hydrocarbon – water systems have been presented in the paper by Hajiw et al. [1]. The one for acid gas-water systems have been adjusted and are given in Table 2. The binary interaction parameter is given by:

$$k_{ij}(T) = \frac{-\frac{1}{2} \times Sum_{PPR78} - \left(\frac{\sqrt{\alpha_i(T)}}{b_i} - \frac{\sqrt{\alpha_j(T)}}{b_j} \right)^2}{2 \frac{\sqrt{\alpha_i(T)\alpha_j(T)}}{b_i b_j}}$$

With sum_{PPR78} defined for non-associating system as

$$Sum_{PPR78} = \sum_{k=1}^{Ng} \sum_{l=1}^{Ng} (\alpha_{ik} - \alpha_{jk})(\alpha_{il} - \alpha_{jl}) A_{kl} \left(\frac{298.15}{T} \right)^{\left(\frac{B_{kl}}{A_{kl}} - 1 \right)}$$

Or for associating systems

$$Sum_{asso} = \sum_{k=1}^{H_2O} (\alpha_{ik} - \alpha_{jk})(\alpha_{iH_2O} - \alpha_{jH_2O})(C_{kH_2O}T^2 + D_{kH_2O}T + E_{kH_2O}) \\ + \sum_{l=1}^{H_2O} (\alpha_{iH_2O} - \alpha_{jH_2O})(\alpha_{il} - \alpha_{jl})(C_{H_2Ol}T^2 + D_{H_2Ol}T + E_{H_2Ol})$$

With $C_{k,H_2O}=C_{H_2O,l}$, $D_{k,H_2O}=D_{H_2O,l}$, $E_{k,H_2O}=E_{H_2O,l}$.

	a_0 bar.L ² .mol ⁻²	b L.mol ⁻¹	C_1	ϵ bar.L.mol ⁻¹	β 10 ³	Temperature Range / K	ΔP %	$\Delta \rho$ %
Water	2.174	0.015	0.639	146.39	68.31	273 – 643	1.1	2.7

Table 1: PR-CPA parameters for pure water according to Hajiw et al. [1]

Comp.	$C_{k,H_2O} / 10^3$ Pa.K ⁻²	$D_{k,H_2O} / 10^6$ Pa.K ⁻¹	$E_{k,H_2O} / 10^9$ Pa
CO ₂	-6.5	5.6	-8.4
H ₂ S	0.067	0.556	0.184

Table 2: Group interaction parameters with water (C_{k,H_2O} , D_{k,H_2O} and E_{k,H_2O})

To predict hydrate phase equilibria, both equations are coupled with the solid solution theory of van der Waals and Platteuw (1959) [3], as developed by Parrish and Prausnitz (1972)[4].

Results and Discussions

Binary systems

To evaluate the accuracy of the GC-PR-CPA model for systems of interest, it is first applied to binary systems containing either acid gas or aromatics with water. Figures 2 and 3 are respectively showing carbon dioxide and hydrogen sulfide solubility in water at different temperatures. For the CO₂-H₂O system, both GC-PR-CPA and PPR78 models are able to represent carbon dioxide solubility over a large range of pressure with 6% and 5% deviation respectively. However, the PPR78 EoS shows larger discrepancies for the H₂S-H₂O system with a relative deviation of 16% against 2% for the GC-PR-CPA EoS.

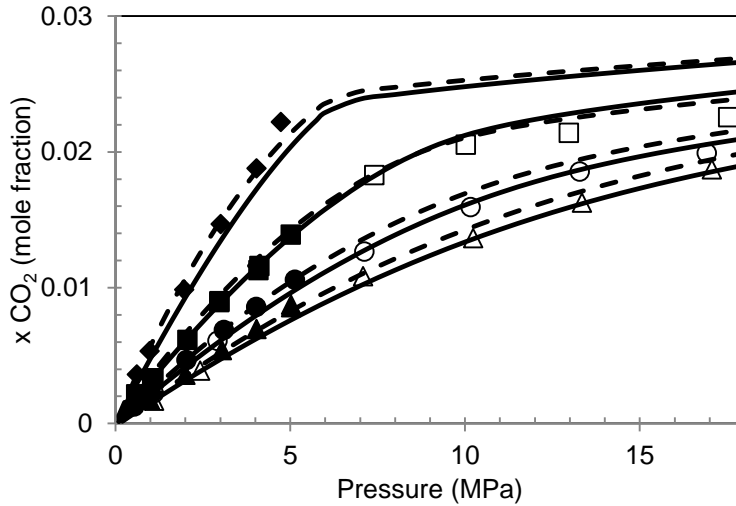


Figure 2: Carbon dioxide solubility in water at 298.15 K (◆, Lucile et al.[7]), 323.15 K (■, Lucile et al. [7] and □ Hou et al. [8]), 348.15 K (●, Lucile et al. [7] and ○ Hou et al. [8]) and 373.15 K (▲, Lucile et al. [7] and Δ Hou et al. [8]). Solid lines: GC-PR-CPA EoS. Dashed lines: PPR78 EoS.

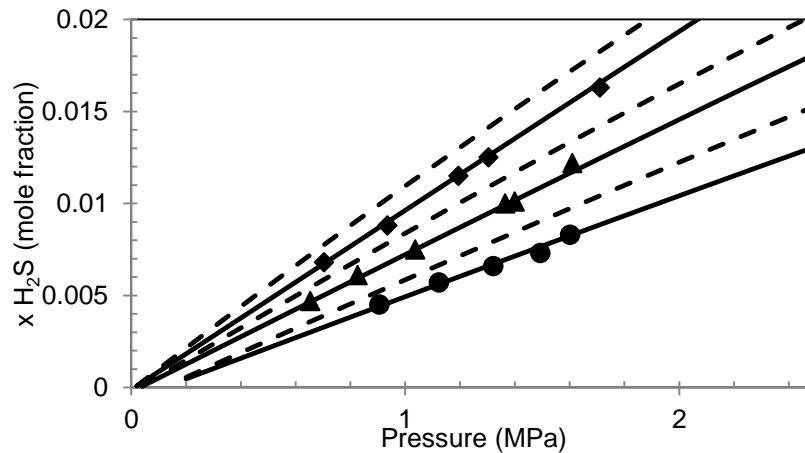


Figure 3: Hydrogen sulfide solubility in water at 323.34 K (◆), 344.33 K (▲) and 377.42 K (●) (Yu et al. [9]). Solid lines: GC-PR-CPA EoS. Dashed lines: PPR78 EoS.

Concerning aromatic solubility in water, limited data are available in the literature, because they are sparingly soluble in water. Therefore, solubility data presented in figures 4 and 5 are given at atmospheric pressure. Both benzene and toluene show a minimum of solubility at 286 K and 289 K respectively. For the benzene-water system, the GC-PR-CPA and PPR78 EoS are in good agreement with experimental data with 2% and 3% deviation respectively. However, the PPR78 EoS does not reproduce the minimum of solubility. It also displays larger discrepancies when representing toluene solubility in water (7% deviation against 1% for the GC-PR-CPA EoS) but shows the minimum of solubility.

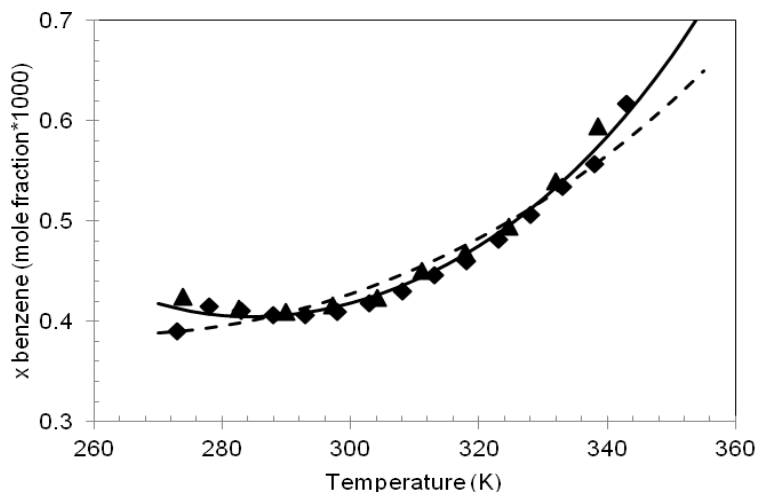


Figure 4: Benzene solubility in water at 0.1 MPa. Experimental data: (▲) (Alexander [10]) and (◆) (Maczynski et al.[11]). Solid lines: GC-PR-CPA EoS. Dashed lines: PPR78 EoS.

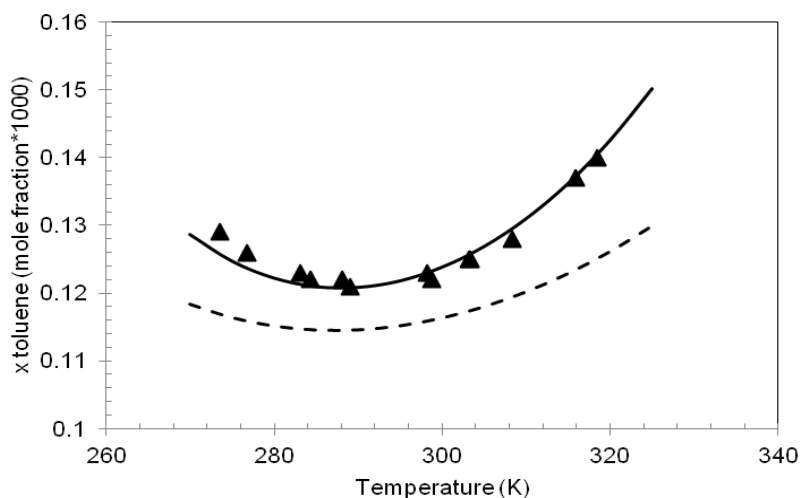


Figure 5: Toluene solubility in water at 0.1 MPa. Experimental data: (◆) (Bohon and Claussen [12]). Solid lines: GC-PR-CPA EoS prediction. Dashed lines: PPR78 EoS.

Multicomponent systems

Two multicomponent systems containing acid gas have been chosen to evaluate the accuracy of the thermodynamic models for more complex systems with water. The first mixture (MIX 1) contains two light hydrocarbons plus acid gas [13]. The second one (MIX 2) is a mixture studied in the GPA Research Project 082 [5]. Their compositions are presented in Table 3. Composition of MIX 1 is close to the one of natural gas before treatment. Both GC-PR-CPA and PPR78 EoS have been applied to calculate the composition of the vapour and liquid phases at 322 K. Deviations are given in Table 4. The phase behaviour of MIX 2 has been experimentally studied in the presence of water at 313 K and 3.6 and 5.6 bar. It exhibits a vapour-liquid-liquid equilibrium that both models are able to represent. As seen in Table 5, they give similar results for the compositions of the hydrocarbon-rich liquid phase (HC liquid) and the vapour phase. For the aqueous phase, the PPR78 EoS shows larger discrepancies in the representation of H₂S solubility but is better for methane solubility. Large deviations between experimental data and predictions can be observed for the aromatics solubility in the aqueous phase because of their small values.

Component	MIX 1 (Ng et al. [17])	MIX 2
Carbon dioxide	18.77	58.80
Hydrogen sulphide	6.25	18.00
Methane	71.21	1.61
Ethane	-	0.187
Propane	3.77	0.093
Cyclopentane	-	0.66
Benzene	-	12.34
Toluene	-	6.82
m-Xylene	-	1.49

Table 3: Composition of acid gases

EoS	Phase	CH ₄	CO ₂	H ₂ S	C ₃ H ₈	H ₂ O
GC-PR-CPA	Liquid	3	5	20	11	0.07
	Vapour	0.5	0.9	8	0.2	38
PPR78	Liquid	7	5	17	17	0.06
	Vapour	0.8	0.7	11	0.4	21

Table 4: Average Absolute Deviation (AAD %) between experimental data for MIX 1 and EoSs at 322 K.

EoS	Phase	CO ₂	H ₂ S	CH ₄	C ₂ H ₆	C ₃ H ₈
GC-PR-CPA	Aq Liquid	18	2	86	25	82
	HC Liquid	24	46	265	117	41
	Vapour	5	17	176	89	22
PPR78	Aq Liquid	16	10	62	41	86
	HC Liquid	23	45	263	116	40
	Vapour	5	16	176	89	23

Table 5: AAD % between experimental data for MIX 1 and EoSs at 3.6 bar and 313 K.

EoS	Phase	C ₅ H ₁₀	C ₆ H ₆	C ₇ H ₈	m-C ₈ H ₁₀	H ₂ O
GC-PR-CPA	Aq Liquid	89	88	96	99	0.47
	HC Liquid	24	18	20	29	
	Vapour	34	35	43	57	
PPR78	Aq Liquid	94	90	97	99	0.41
	HC Liquid	24	17	20	29	
	Vapour	33	35	43	57	

Table 6: AAD % between experimental data for MIX 2 and EoSs at 3.6 bar and 313 K.

Hydrate stability in presence of free water

Different mixtures with acid gases in presence or not of aromatic liquids have studied and compared to see the influence of aromatics on hydrate phase equilibria of acid gases in the GPA Research Project 082 [5]. Results for some selected mixtures are presented herein (Table 7). Experimental measurements and predictions with both models are plotted in Figure 6.

The PPR78 and GC-PR-CPA models are able to predict hydrate dissociation curve for the three mixtures presented within the experimental errors.

Hydrate stability zone of MIX 4 is very close of the one of pure CO₂. The presence of H₂S (MIX 3) promotes hydrates formation and displaces the hydrate dissociation curve to higher temperatures. Addition of aromatic compounds either promotes (no or low H₂S concentration in the acid gas mixture) or inhibit the hydrate stability zone.

Component	MIX 3	MIX 4	MIX 5
CO ₂	46.5	99.0	50.61
H ₂ S	50.0	-	22.03
Methane	3.5	0.85	1.66
Ethane	-	0.10	0.18
Propane	-	0.05	0.10
Cyclopentane	-	-	1.79
Benzene	-	-	0.76
Toluene	-	-	8.13
m-Xylene	-	-	14.74

Table 7: Compositions (mole %) of mixtures for hydrate measurements

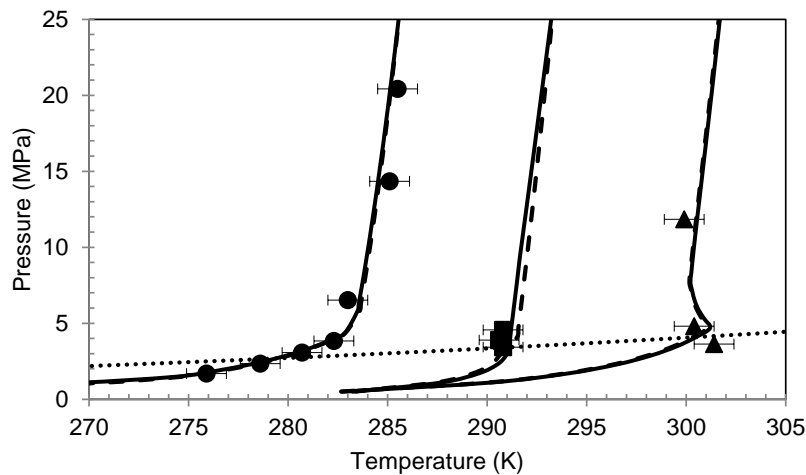


Figure 6: Hydrate dissociation points for different acid gas mixtures. ▲ MIX 3, ● MIX 4 and ■ MIX 5 [18]. Solid lines: GC-PR-CPA EoS. Dashed lines: PPR78 EoS. Dotted lines: PT envelope of MIX 5.

Conclusions

Acid gas injection is the preferential method for dealing with unwanted acid gases. However, mixtures obtained after treatment contains different impurities including aromatics. Considering the different compositions of mixtures that can be obtained, as well as the operating conditions, reliable thermodynamic models are of great importance. The predictive GC-PR-CPA model is able to predict phase behaviours (VLE, VLLE, LLE and hydrate stability zone) of multi-component systems.

From the results obtained in the GPA Research Project 082 [5], it has been seen that the presence of aromatics has small impact on the hydrate stability zone, but it can be of great importance when considering the compression step before injection. Indeed, there is likely that a liquid phase appears at conditions usually applied for gas compression. It would be interesting to extend experimental measurements to transport properties such as density, to see the impact of aromatics and to evaluate thermodynamic models on their ability to predict such data.

Acknowledgment

The authors wish to gratefully acknowledge Eric Boonaert and Alain Valtz for their expertises and technical advices.

References

- [1] M. Hajiw, A. Chapoy, C. Coquelet, Hydrocarbons - water phase equilibria using the CPA equation of state with a group contribution method, *Can. J. Chem. Eng.* 93 (2015) 432–442. doi:10.1002/cjce.22093.
- [2] M. Hajiw, A. Chapoy, C. Coquelet, G. Lauermaun, Prediction of methanol content in natural gas with the GC-PR-CPA model, *J. Nat. Gas Sci. Eng.* 27 (2015) 745–750. doi:10.1016/j.jngse.2015.09.021.
- [3] J.H. van der Waals, J.C. Platteeuw, Clathrate solutions, *Adv. Chem. Phys.* 2 (1958) 1–57. doi:10.1002/9780470143483.ch1.
- [4] W.R. Parrish, J.M. Prausnitz, Dissociation Pressures of Gas Hydrates Formed by Gas Mixtures, *Ind. Eng. Chem. Process Des. Dev.* 11 (1972) 26–35. doi:10.1021/i260041a006.
- [5] M. Hajiw, E. Boonaert, A. Valtz, E. El Ahmar, A. Chapoy, C. Coquelet, Impact of Aromatics on Acid Gas Injection, *GPA Res. Rep.* 230 (2016) 1–111.
- [6] X. Xu, J.N. Jaubert, R. Privat, P. Duchet-Sucaux, F. Braña-Mulero, Predicting Binary-Interaction Parameters of Cubic Equations of State for Petroleum Fluids Containing Pseudo-components, *Ind. Eng. Chem. Res.* 54 (2015) 2816–2824. doi:10.1021/ie504920g.
- [7] F. Lucile, J. Serin, D. Houssin, P. Arpentinier, Solubility of Carbon Dioxide in Water and Aqueous Solution Containing Sodium Hydroxide at Temperatures from (293.15 to 393.15) K and Pressure up to 5 MPa: Experimental Measurements, *J. Chem. Eng. Data.* 57 (2012) 784–789.
- [8] S.-X. Hou, G.C. Maitland, J.P.M. Trusler, Measurement and modeling of the phase behavior of the (carbon dioxide+water) mixture at temperatures from 298.15K to 448.15K, *J. Supercrit. Fluids.* 73 (2013) 87–96. doi:10.1016/j.supflu.2012.11.011.
- [9] et al. Yu, Q., Vapor liquid equilibria of hydrogen sulfide - water system, *Chem. Eng.* 4 (1980) 1–7.
- [10] D.M. Alexander, The Solubility of Benzene in Water, *J. Phys. Chem.* 63 (1959) 1021–1022. doi:10.1021/j150576a608.
- [11] A. Maczynski, V. Editor, IUPAC-NIST Solubility Data Series . 81 . Hydrocarbons with Water and Seawater — Revised and Updated . Part 2 . Benzene with Water and Heavy Water, 34 (2005). doi:10.1063/1.1790006.
- [12] R.L. Bohon, W.F. Claussen, The Solubility of Aromatic Hydrocarbons in Water, *J. Am. Chem. Soc.* 73 (1951) 5883–5884.
- [13] H.-J. Ng, C.-J. Chen, H. Schroeder, Water Content of Natural Gas Systems Containing Acid Gas, RR-174 (2001).